Monthly Notices
of the
ROYAL ASTRONOMICAL SOCIETY

Mon. Not. R. Astron. Soc. **414,** 2629–2641 (2011) doi:10.1111/j.1365-2966.2011.18584.x

Effect of magnetic activity saturation in chromospheric flux–flux relationships

R. Martínez-Arnáiz,⋆ J. López-Santiago, I. Crespo-Chacón and D. Montes†

Departamento de Astrofísica, Facultad de Ciencias Físicas, Universidad Complutense de Madrid, E-28040 Madrid, Spain

Accepted 2011 February 22. Received 2011 February 21; in original form 2010 December 21

ABSTRACT

We present a homogeneous study of chromospheric and coronal flux–flux relationships using a sample of 298 late-type dwarf active stars with spectral types F to M. The chromospheric lines were observed simultaneously in each star to avoid spread as a result of long-term variability. Unlike other works, we subtract the basal chromospheric contribution in all the spectral lines studied. For the first time, we quantify the departure of dMe stars from the general relations. We show that dK and dKe stars also deviate from the general trend. Studying the flux–colour diagrams, we demonstrate that the stars deviating from the general relations are those with saturated X-ray emission and we show that these stars also present saturation in the Hα line. Using several age spectral indicators, we show that these are younger stars than those following the general relationships. The non-universality of flux–flux relationships found in this work should be taken into account when converting between fluxes in different chromospheric activity indicators.

Key words: stars: activity – stars: chromospheres – stars: flare – stars: late-type – solar neighbourhood.

1 INTRODUCTION

The study of stellar chromospheric and coronal emission is fundamental for an understanding of the outer layers of late-type stars. A number of problems can be addressed with activity-based studies, such as the generation of stellar magnetic fields by dynamo processes or the nature of coronal heating and its relation to stellar activity. Determining the magnetic activity level, per se, is also important in other research topics, such as accurately measuring radial velocity (e.g. Saar & Donahue 1997) or detecting transiting planets (e.g. Henry et al. 1997). Another example that has interested the astronomy community for the past few years is the effect of magnetic activity on the formation and evolution of planets and their atmospheres (e.g. Cuntz, Saar & Musielak 2000) and, in a more general context, the evolution of overall stellar magnetic activity with age.

When the (sometimes substantial) contribution from the acoustically driven basal atmosphere is subtracted from the observed emission, power-law relationships are found between the excess flux in different activity indicators (see Schrijver & Zwaan 2000). The first empirical flux–flux relationships were used to compare fluxes in chromospheric and coronal lines with the aim of studying the magnetic structure of stellar atmospheres (Schrijver 1987; Rutten et al. 1991). Subsequent studies analysed the relationship among different chromospheric activity indicators, such as Ca II H & K lines and H_α (Strassmeier et al. 1990; Robinson, Cram & Giampapa 1990; Montes et al. 1995b,1996a,b; Cincunegui, Díaz & Mauas 2007) or the Ca II infrared triplet (IRT; Thatcher & Robinson 1993; López-Santiago et al. 2005; Busà et al. 2007; Martínez-Arnáiz et al. 2010, hereafter MA10). Basically, Montes et al. (1995b); Montes et al. (1996a,b) and Strassmeier et al. (1990) included mostly binary (in many cases also evolved) stars. López-Santiago et al. (2005), Cincunegui et al. (2007) and MA10 based their studies on single stars with spectral types F to K. It is important to mention that there is no standard technique to correct for the photospheric contribution among the studies mentioned. This makes the comparison between data acquired by different researches difficult. Besides, in many of the previous studies, the observations of the two activity indicators were not simultaneous. This fact introduces an important scatter in the flux–flux relationships because of the intrinsic variability of stellar magnetic activity. To date, these power-law relationships have been found to be independent of effective temperature or of stellar luminosity class for classes II–V (provided that stars beyond mid-M type are excluded).

Some previous studies found that M dwarfs presented a slight departure from the main flux–flux relationships in some spectral lines. In particular, this departure was found for emission-line M dwarfs when comparing chromospheric indicators with

⋆E-mail: rma@astrax.fis.ucm.es

†Based on observations collected with the FEROS spectrograph at the 2.2-m telescope at the European Organization for Astronomical Research in the Southern Hemisphere, Chile [Programme: 074.D-0016(A).].

© 2011 The Authors
Monthly Notices of the Royal Astronomical Society © 2011 RAS

Downloaded from http://mnras.oxfordjournals.org/ at Universidad Complutense de Madrid on February 9, 2016

transition-region ones (Oranje 1986; Rutten et al. 1989; Schrijver & Zwaan 2000) or with the coronal soft X-ray emission (Schrijver & Rutten 1987). However, all the departures from the general flux–flux relationships found in these studies were (i) restricted to dMe stars and (ii) restricted to the comparison between the chromosphere and outer layers (transition region and corona). Besides, the fact that the coronal X-ray and transition-region ultraviolet (UV) observations were not simultaneous to those of the chromosphere, introduced an important source of scatter as a result of the intrinsic variation of active stars (Schrijver, Dobson & Radick 1992). Later, López-Santiago et al. (2005) showed that some active late-K- and M-type stars deviated from classical Hα–Ca II flux–flux relationships. They tentatively identified these with flare stars. The sample of M dwarfs in all these studies has been systematically biased towards emission-line stars. Therefore, these studies could not conclude whether this departure from the main flux–flux relationships was restricted to late-type stars with clear emission-line characteristics or whether it was common to a larger group of late-K- and M-type stars. The main objective of this work is to check which types of star depart from the main flux–flux relationships when two chromospheric indicators are compared. In addition, we aim to properly quantify this departure using chromospheric fluxes that are appropriately corrected from the atmospheric basal contribution. By so doing, we will provide unique information on the validity of the use of such relationships when trying to convert between fluxes in different lines.

For this research, we used high-resolution optical echelle spectra. A noteworthy advantage of echelle spectra is that they cover a large fraction of the optical spectrum simultaneously. Therefore, they allow a simultaneous observation of all the activity indicator lines present in this spectral range, avoiding the spread in the relations caused by the temporal variability of activity levels. This fact implies a significant improvement of the flux–flux relationships with respect to those previously obtained, because most of the latter were built by using activity diagnostics that were not measured simultaneously. In addition, the chromospheric fluxes obtained from this method are corrected for the basal chromospheric emission.

Details on the technical information of the observations and data reduction are given in Section 2. In Section 3 we describe the analysis of the observations and the obtained excess emission equivalent widths, excess surface fluxes and X-ray luminosities and fluxes. Finally, Sections 4 and 5 are devoted, respectively, to a discussion of the results and the conclusions of this work.

2 DATA SELECTION AND REDUCTION

The present study is based on high-resolution echelle spectra. The total sample comprises 298 main-sequence, late-type (spectral types F to M), single, active stars. We used data from López-Santiago et al. (2010, hereafter LS10) for 144 stars and data from MA10 for 173.[1] The former sample is mainly formed by main-sequence stars but also includes some star members of young associations and kinematic groups. The 16 binaries of that sample have not been included in our study. The MA10 sample is formed only by main-sequence single stars. Thus, all the active stars in this sample have been included in our study. We refer the reader to the works mentioned for a detailed explanation on the observing runs, telescopes and instruments they used, as well as the characteristics of their spectra. We also note that there are 22 common stars between LS10 and MA10. After eliminating all binaries in LS10 and cross-correlating this sample with MA10, we obtained a total of 279 late-type stars. We note that the MA10 and LS10 samples are complementary in terms of emission levels: while the former includes mainly low-activity stars, the latter is principally formed by young active stars. This fact is important, bearing in mind that we aim to obtain precise flux–flux relationships and to determine whether they hold for all spectral types and activity levels.

Given that previous studies showed a peculiar behaviour for some late-K and M stars (López-Santiago et al. 2005), and that the MA10 and LS10 samples only include a small number of these types of stars, we considered it necessary to increase the number of these types of stars in the total sample. To complete the sample and increase the ratio of late-K and M stars, we obtained high-resolution echelle spectra of 21 late-K and M stars, some of them well-known members of young associations and moving groups. Bearing in mind that previous studies suggested that those stars deviating from the main flux–flux relationships were only those with emission features, the stars chosen to increase the sample are late-K and M types with and without such features. The chosen stars were also selected on the grounds of their known activity levels and youth. Only those stars with no signatures of accretion that could, eventually, affect chromospheric emission have been used (see Section 4.1). The observations of this new sample of late-K and M stars were carried out at the European Southern Observatory (ESO; La Silla, Chile) in 2005 February with the fibre-fed extended range optical spectrograph (FEROS) linked to the Cassegrain focus of the 2.2-m telescope, with the CCD 2048 $\times$ 4096 (0.15 μm pixel^{-1}). This configuration provides observations within the spectral range 3500–9200 Å with a resolution of 48 000 (reciprocal dispersion ranging from 0.03 to 0.09 Å pixel^{-1} from the red to the blue region of the spectrum) in a total of 39 orders. This campaign will be referred as the FEROS05 observing run hereafter. Preliminary results for some of the stars observed in this observing run are found in Montes et al. (2007, 2008). We note that there is one star in common with LS10 and one in common with MA10.

We used the reduction procedures in the IRAF[2] packages and the standard method: bias and dark subtraction, flat-field division, cosmic ray correction, scattered light subtraction and optimal extraction of the spectra. Th–Ar lamps were used to perform the wavelength calibration. Finally, all the spectra were normalized by using a cubic spline polynomial fit to the observed continuum. We note that both the reduction process and data analysis for the stars in the FEROS05 observing run were completely analogous to those used by LS10 and MA10 in their respective works. Together with the fact that the technique used to obtain chromospheric fluxes (see Section 3.1) was the same, this ensures the compatibility of all the data used in this study.

The complete stellar sample contains 298 stars. The spectral-type distribution of the whole sample is: 17 F-type stars, 60 G-type stars, 182 K-type stars and 39 M-type stars. Fig. 1 shows the spectral-type distribution for LS10, MA10 and the FEROS05 observing run.

3 DATA ANALYSIS

As mentioned in Section 1, (power-law) flux–flux relationships between chromospheric features are found only when basal chromospheric activity is subtracted. This basal flux is common to active

[1] We note that we have only used data for the stars classified as active.

[2] IRAF is distributed by the National Optical Astronomy Observatories, which are operated by the Association of Universities for Research in Astronomy, Inc., under cooperative agreement with the National Science Foundation.

Downloaded from http://mnras.oxfordjournals.org/ at Universidad Complutense de Madrid on February 9, 2016

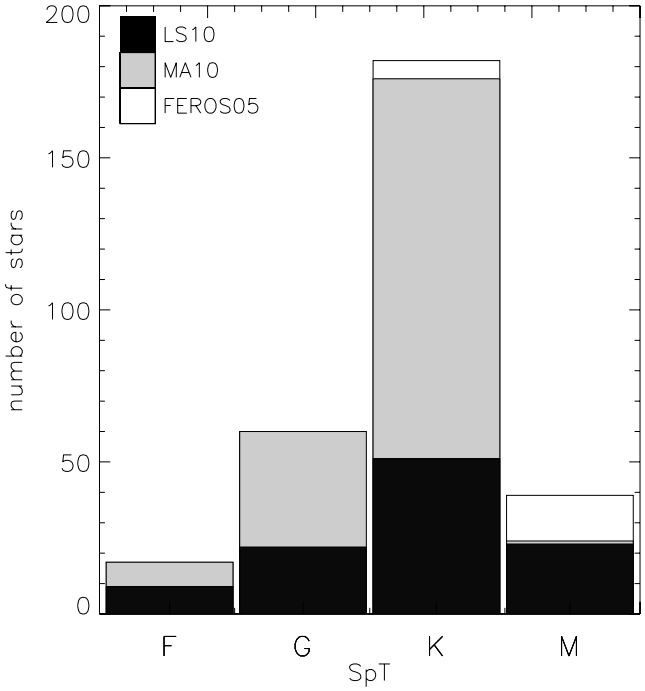

Figure 1. Spectral-type distribution of the complete stellar sample. Note that all the stars in the sample are active.

and non-active stars. Therefore, it is subtracted from the active star when using a non-active star as a reference for the spectral subtraction instead of theoretical synthetic photospheric spectra (see MA10 and LS10 for details). We used the same technique to reveal and measure the equivalent widths of chromospheric lines in the FEROS05 stars. Then, we converted equivalent widths to fluxes using empirical calibrations. In the following subsections, we give the details of the analysis process.

3.1 Spectral subtraction technique: excess equivalent width

The spectral subtraction technique (see, for example, Montes et al. 1995a, 2000) is an unparalleled method to obtain the chromospheric contribution to the spectrum of a star. It permits the subtraction of the underlying photospheric contribution from the stellar spectrum. In this way, the spectral emission that originated at the chromosphere can be studied in detail. When the spectrum of a non-active star with similar spectral type, gravity and chemical composition is used, the basal chromospheric flux is also subtracted (see MA10). Thus, any theoretical or semi-empirical calibration to subtract basal emission is avoided. As mentioned above, this is important because power-law relationships between the flux in different activity indicators only hold when the acoustically driven basal chromospheric emission is eliminated (Schrijver & Zwaan 2000).

For this work, we artificially constructed synthesized spectra using the program JSTARMOD.[3] The synthesized spectrum consists of the sum of rotationally broadened, radial-velocity shifted, and weighted spectra of non-active stars, which are chosen to match the spectral types and luminosity classes of the components of the active star under consideration. In this work, the non-active stars used as reference stars for the spectral subtraction were observed during the same observing run as their respective active stars. Once computed, the synthesized spectrum was subtracted from that of the target star to obtain a spectrum of the non-basal chromospheric contribution alone. Excess equivalent widths of the activity indicators were measured in this subtracted spectrum. To estimate the errors in the measured equivalent widths, we followed López-Santiago et al. (2003) and considered JSTARMOD's typical internal precisions (0.5–2 km s^{-1} in velocity shifts and ±5 km s^{-1} in projected rotational velocities, $v \sin i$), the rms in regions outside the chromospheric features (typically 0.01–0.03) and the standard deviations. The estimated errors for relatively strong emitters are in the range 10–20 per cent, but for low-activity stars errors are larger. Taking into consideration that the signal-to-noise ratio (S/N) is lower (higher rms) in the blue spectral region, errors in the chromospheric features at these wavelengths are larger. We refer the reader to LS10 and MA10 for a description of the stars used as references. In Table 1, we list the stars used as references for the FEROS05 stars.

[3] JSTARMOD is a modified version of the FORTRAN code STARMOD developed at Penn State University (Huenemoerder & Barden 1984; Barden 1985). The modified code, implemented by J. López-Santiago, admits as input echelle spectra obtained with a CCD with more than 2048 pixels in the horizontal and/or vertical directions.

Table 1. Stars used as reference to subtract the photospheric contribution to the spectrum of the FEROS05 stars.

Name	Other name	SpT	$B-V$	$v \sin i$
			km s^{-1}	
HIP 83591	HD 154363	K5V	1.139	3.70[a]
HIP 62687	HD 111631	K7	1.348	–
HIP 60661	GJ 466	M0V	1.153	–
HIP 25878	HD 36395	M1.5V	1.383	1.0[b]
HIP 51317	GJ 393	M2	1.448	1.1[b]
HIP 61706	GJ 480	M3	1.470	0.8[b]
HIP 36208	GJ 273	M3.5	1.438	0.0[b]

[a]LS10.
[b]Jenkins et al. (2009).

3.2 Excess surface fluxes

Fluxes were derived for each of the activity indicators from its measured equivalent width (EW_l) by using the continuum flux

$$F_{s,l} = EW_l F^{cont}_{s,l} \Longrightarrow \log F_{s,l} = \log(EW_l) + \log(F^{cont}_{s,l}). \quad (1)$$

Here, the continuum flux, $F^{cont}_{s,l}$, is dependent on the wavelength and must therefore be determined for the region where the activity indicator line is. We used the empirical relationships between $F^{cont}_{s,l}$ and colour index, $B-V$, derived by Hall (1996) to compute $F^{cont}_{s,l}$ in the Ca II H & K, Hα and Ca II IRT regions. We note that the aforementioned relationships are linear for the spectral-type range of our sample stars with the exception of the calibration for the Hα region, for which Hall (1996) found small deviations from the linear trend for stars with $B-V \geq 1.4$. This implies that, in principle, the calibration for the Hα region may not be valid for those stars cooler than M2/M3. We have explored the possibility of using the χ-factor correction (Walkowicz, Hawley & West 2004; West, Walkowicz & Hawley 2005; West & Hawley 2008), which permits the derivation of L_{H_α}/L_{bol} directly from the measured equivalent widths of the emission lines and the colour index $B-V$ of the star by using

$$L_{H_\alpha}/L_{bol} = \chi \times EW_{H\alpha}. \quad (2)$$

To test whether the χ-factor correction and that based on the Hall (1996) calibration are consistent, we have compared the values of L_{H_α}/L_{bol} obtained with both methods for M stars of the

Downloaded from http://mnras.oxfordjournals.org/ at Universidad Complutense de Madrid on February 9, 2016

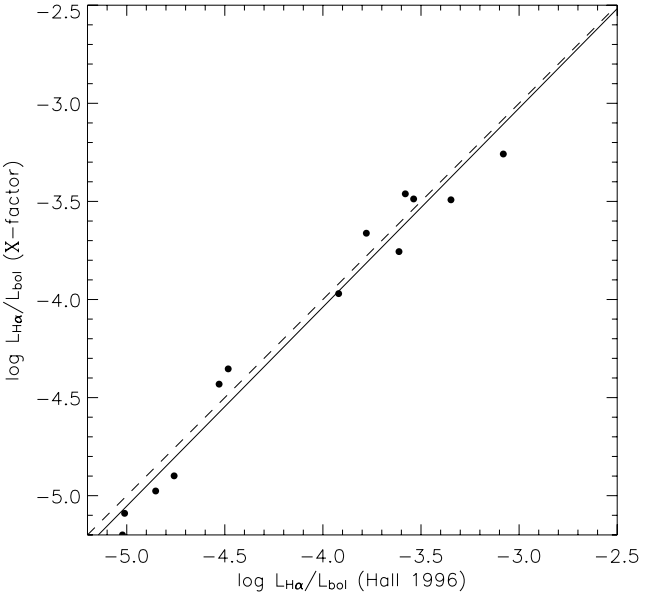

Figure 2. Comparison between Hα luminosities obtained using the χ-factor correction and that in Hall (1996). The dashed line is the one-to-one relation, while the continuous line is the linear fit to the data.

FEROS05 campaign (see Fig. 2). For these stars, bolometric luminosities ($L_{\rm bol}$) were determined using a zero-age main-sequence (ZAMS) calibration. The correlation between both results is clear: the linear regression equation is

$$(L_{\rm H_\alpha}/L_{\rm bol})_{\chi-\rm factor} = 1.01(L_{\rm H_\alpha}/L_{\rm bol})_{\rm Hall\,1996} + 0.02\,(R = 0.98). \quad (3)$$

Note that the maximum deviation in Fig. 2 is 0.15 dex, which is within the dispersion range in the relations found by Hall (1996) and those presented in West & Hawley (2008). The fact that the obtained linear fit is compatible to the one-to-one relation implies that the Hall (1996) calibrations for the continuum flux in the Hα region can also be used for M0–M4 stars with the same level of confidence as the χ-factor correction. To ensure a homogeneous analysis of the data and to obtain fluxes instead of luminosities, we have used the Hall (1996) calibration for all stars.

In Table A3, we give the absolute flux at the stellar surface and its error for the late-K and M stars of the FEROS05 observing run. We refer the reader to LS10 and MA10 for a compilation of the fluxes of the rest of the stars.

3.3 X-ray fluxes and luminosities

X-ray flux is a direct measure of stellar activity because it is unlikely to include contributions from other sources, such as the basal atmosphere (Rutten et al. 1991; Schrijver et al. 1992). Therefore, in addition to the optical data, we searched for X-ray counterparts of the stars in our sample in the *ROSAT* All-Sky Survey (RASS) catalogue. For this purpose, we followed López-Santiago, Micela & Montes (2009). We cross-correlated our total stellar sample with the *ROSAT* All-Sky Survey Bright Source Catalogue (RASS-BSC) and the Faint Source Catalogue (RASS-FSC) using a search radius of 30 arcsec to account for the *ROSAT* X-ray object coordinate determination accuracy. We found 243 counterparts for the sample of 298 stars.

To determine the X-ray fluxes, we used the count rate to energy flux conversion factor (*CF*) relation found by Schmitt, Fleming & Giampapa (1995):

$$CF = (5.30 \times HR + 8.31) \times 10^{-12}\ \rm erg\,cm^{-2}\,counts^{-1}. \quad (4)$$

Here, *HR* is the hardness ratio of the star in the *ROSAT* energy band 0.1–2.4 keV, defined as $HR = (H - S)/(H + S)$ with H and S being the counts in the detector channels 11–49 and 52–201, respectively. X-ray fluxes were determined by multiplying the *CF* value by the count rate[4] of the sources in the same band. Note that the fluxes determined in this way are observed fluxes but not surface fluxes. Fluxes were then transformed into luminosities using the distances from the star to the Earth. Because the *CF* and the count rate (*CR*) are defined for the *ROSAT* energy band 0.1–2.4 keV, the X-ray luminosity $L_{\rm X}$ is also integrated in this band.

To obtain surface X-ray fluxes, we used the computed luminosities and the stellar radius. As the stars in the sample are dwarfs (see LS10, MA10 and Table A1), the radii were estimated by using a ZAMS calibration.

The number of matches between our sample and the RASS decreases with increasing distance. For instance, López-Santiago et al. (2009) observed that, for their sample, at $d \leq 40$ pc, approximately 70 per cent of the stars were cross-identified, while at $d \leq 50$ pc, only half of them had an RASS counterpart. This suggests that some X-ray emitters at large distances are lost as a consequence of the flux limit of the RASS, producing a bias in our X-ray sample. Note that the MA10 sample is limited to 25 pc and this effect should be negligible.

4 FLUX–FLUX RELATIONSHIPS

In the following, we address the subject of flux–flux relationships from a classical point of view and make no distinction between stars.

4.1 Chromospheric flux–flux relationships

In Figs 3 and 4, we compare pairs of fluxes of different chromospheric lines for all the stars in our sample. For those stars observed more than once, we plot the median value determined by us with all the observations and an error bar representing the maximum deviation from it. Power-law relationships between pairs of lines have been determined by fitting the data to a relation of the type

$$\log F_1 = c_1 + c_2 \log F_2, \quad (5)$$

where F_1 and F_2 are the fluxes of two different lines and c_1 and c_2 are the fitting parameters. We used the method explained in Isobe et al. (1990) to determine c_1, c_2 and their errors. The bisector of the two possible ordinary least-squares regressions (Y on X and X on Y) was determined in each case. The ordinary least-squares bisector regression is the best solution when the goal is to estimate the underlying functional relation between the variables (see Isobe et al. 1990, for a complete study of the problem).

In Table 2 we present the results for c_1 and c_2. This table also lists the values of the slope (c_2) previously obtained in different studies by other authors (Schrijver et al. 1989; Montes et al. 1995b; 1996a,b; López-Santiago 2005; MA10). Comparing columns 5 and 7 in Table 2, we observe that the values obtained for the linear fit of the data in this work are compatible, taking uncertainties into account, with those previously reported for single F, G and early-K stars for all chromospheric indicators. It is important to mention that

[4] The count rate in the *ROSAT* energy band (0.1–2.4 keV).

Downloaded from http://mnras.oxfordjournals.org/ at Universidad Complutense de Madrid on February 9, 2016

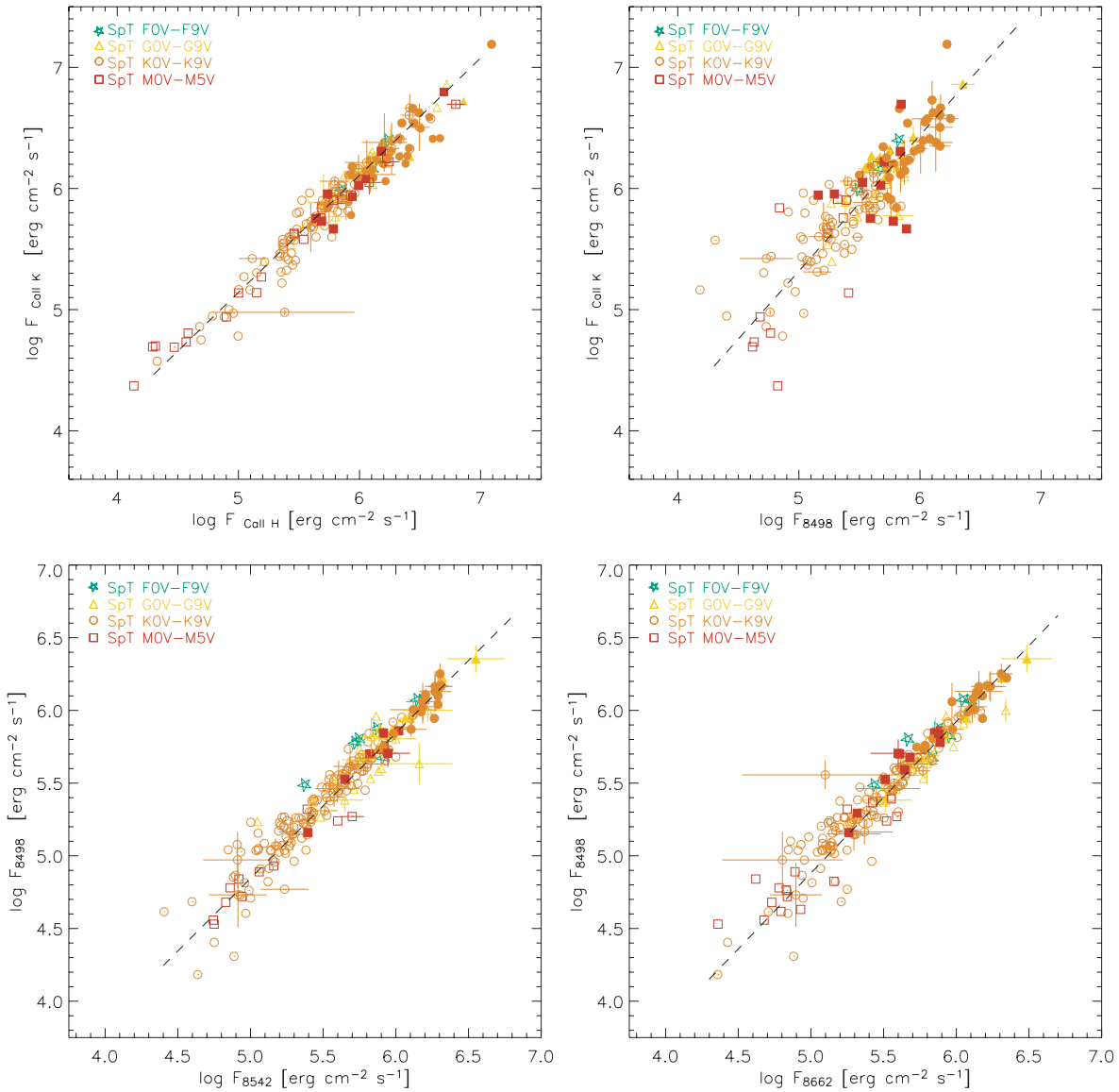

Figure 3. Flux–flux relationships between calcium lines (Ca II H & K and Ca II IRT). Green stars represent F-type stars, yellow triangles G-type stars, orange circles K-type stars and red squares M-type stars.

while this study is based on single active stars, Montes et al. (1995a) focused on active binary stars. However, the differences obtained in the latter cases are no more noticeable than those obtained when we compare the results obtained in this work and other studies based on single stars.

The values obtained for the slopes in the relationships between pairs of logarithmic fluxes follow the trend that has previously been reported (i.e. the larger the difference in atmospheric height at which the compared lines form, the larger the value of the slope). This result has been obtained before, using not only chromospheric indicators (Montes et al. 1996a), but also the transition region (Oranje 1986; Schrijver & Zwaan 1991; Montes et al. 1996a) and coronal diagnostics (Schrijver et al. 1989; Montes et al. 1996a).

It is important to mention that after measuring excess equivalent widths, we applied the Hα *EW* criterion (Barrado y Navascués & Martín 2003) to ensure that no stars with an accretion disc were included. None of the stars in the sample had Hα above the threshold. Thus, we can ensure that the measured equivalent widths (and computed fluxes) are not affected by non-chromospheric Hα emission.

4.2 Chromospheric–coronal connection

In addition to the flux–flux relationships between chromospheric activity diagnostics, we have obtained empirical power laws between chromospheric and coronal (as given by X-rays) fluxes. Details on the search strategy and the conversion from count rate to X-ray fluxes are given in Section 3.3. In Fig. 5 we present the empirical relationships between X-ray surface flux and Hα (left panel) and Ca II λ8498 Å (right panel). Table 2 includes the linear regression parameters for these relationships.

Because of the flux limit of the RASS, our sample of cross-matched X-ray sources is incomplete for low X-ray surface fluxes. For instance, at 20 pc, RASS is incomplete for

Downloaded from http://mnras.oxfordjournals.org/ at Universidad Complutense de Madrid on February 9, 2016

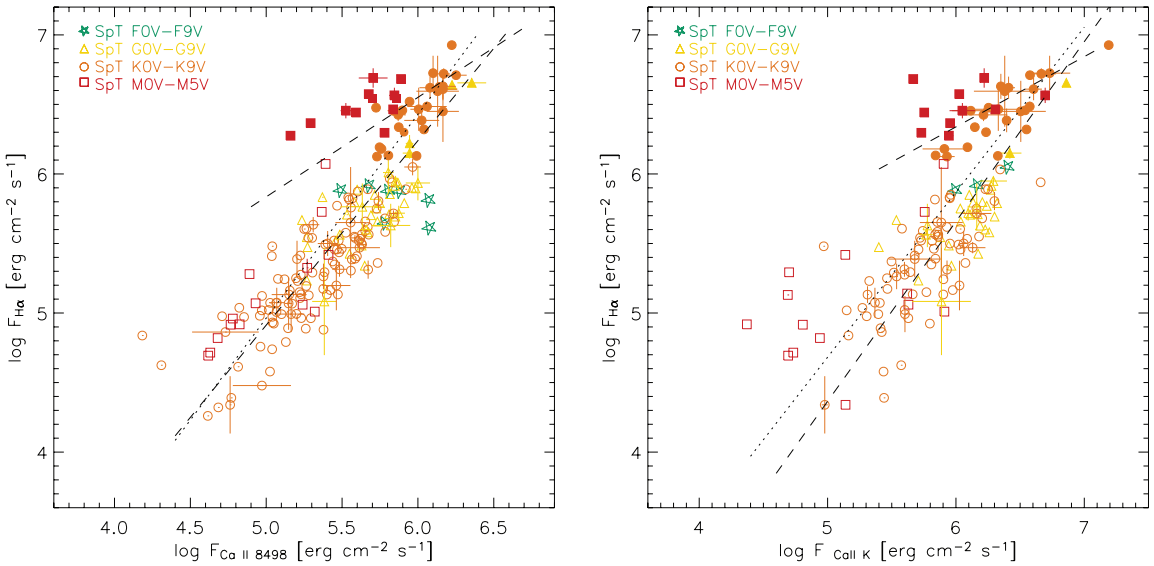

Figure 4. Flux–flux relationships between Hα and Ca II IRT λ8498 Å (left) and Ca II K (right). Green stars represent F-type stars, yellow triangles G-type stars, orange circles K-type stars and red squares M-type stars. Filled symbols are used for those stars that appear in the upper branch Hα versus $B - V$ (those stars above the gap in Fig. 7, and thus younger). The dotted line corresponds to the fit of all data whereas the dashed lines represent the fit for each population of stars.

Table 2. Linear fit coefficients for each flux–flux relationship found in this paper and in previous studies.

		This work		Other studies
$\log F_1$	$\log F_2$	c_1	c_2	Power-law exponent
Chromosphere–chromosphere				
Ca II K	Ca II H	0.30 ± 0.17	0.97 ± 0.03	1.00^a, 0.99^b
Ca II K	Ca II IRT (λ8498 Å)	-0.29 ± 0.51	1.12 ± 0.09	1.01^b
Ca II IRT (λ8498 Å)	Ca II IRT (λ8662 Å)	-0.13 ± 0.19	1.00 ± 0.03	–
Ca II IRT (λ8498 Å)	Ca II IRT (λ8542 Å)	-0.33 ± 0.21	1.04 ± 0.03	1.01^b
Hα	Ca II IRT (λ8498 Å)	-2.36 ± 0.35	1.46 ± 0.06	–
Hα	Ca II K	-1.25 ± 0.52	1.19 ± 0.08	1.13^{ac}, 0.95^b, 1.12^d
Corona–chromosphere				
X	Hα	-2.19 ± 0.41	1.48 ± 0.07	2.11^d
X	Ca II IRT (λ8498 Å)	-4.28 ± 0.77	1.98 ± 0.13	–

[a]López-Santiago et al. (2005).
[b]MA10.
[c]Montes et al. (1995b).
[d]Montes et al. (1996a,b).

$L_X \leq 10^{28}$ erg cm^{-2} s^{-1} (see López-Santiago et al. 2009, and Section 3.3), which corresponds to $\log F_X \sim 5.5$ (with flux in cgs) for a K dwarf. Note that some stars cross-correlated with an RASS counterpart show lower values of $\log F_X$. However, we determined the relationships in the range $\log F_X > 5.5$ to prevent any error in the determination of the relations because of this bias. In Fig. 5, the bias toward low F_X is clear, as only some stars with $\log F_X \sim 5$ are present.

In general, the dispersion in these relationships is larger than that obtained between chromospheric lines. As mentioned in Section 3.3, the uncertainties in the stellar radii estimations affect the X-ray surface flux determination and contribute to the dispersion observed in Fig. 5. Another source of dispersion is the time variability of activity levels. While all the chromospheric indicators were obtained simultaneously, X-ray observations were performed at a different time. This result illustrates the importance of using simultaneous observations to build flux–flux relationships and to avoid the time variability of activity levels.

Contrary to what was observed for the chromospheric flux–flux relationships, our result with X-ray emission is different from that obtained by Montes et al. (1996a). In the latter study, the authors used only binary systems for their study, many of them with both stars emitting in X-rays and/or in optical chromospheric lines. On some occasions, they could separate both components in their optical spectra, but never in X-rays (the authors used data from the *ROSAT* not corrected for binarity). This introduces systematical uncertainties and much more spread in the relationships. Therefore, the difference between our determined value for the slope of the coronal–chromospheric flux relationships and that found by Montes et al. (1996a) does not apply because of the systematic uncertainties introduced by determining X-ray emission from binary stars in the latter study.

Downloaded from http://mnras.oxfordjournals.org/ at Universidad Complutense de Madrid on February 9, 2016

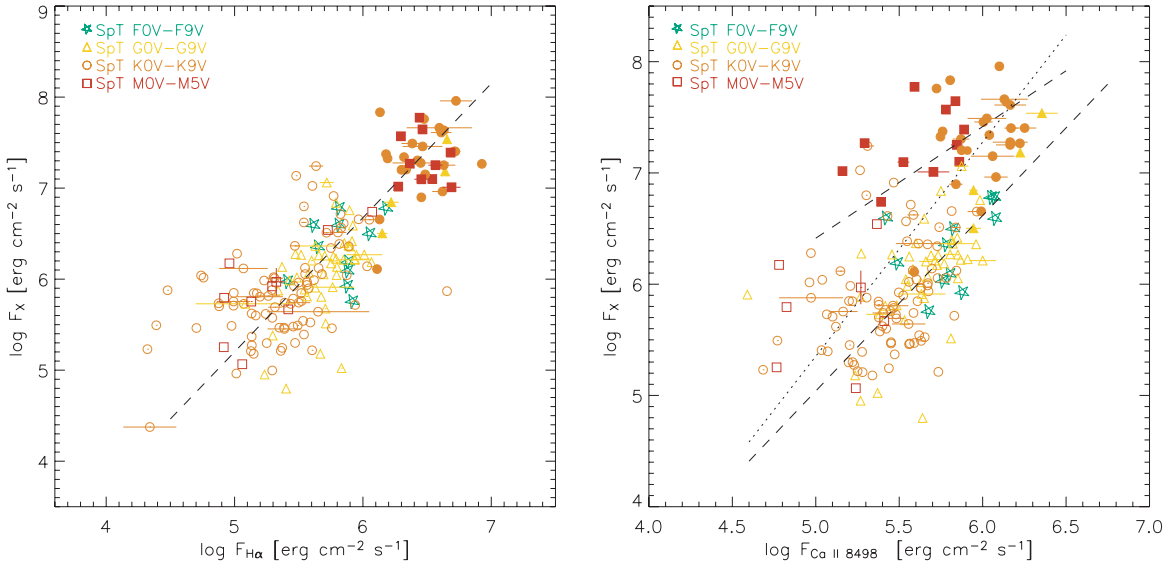

Figure 5. Relationships between logarithmic X-ray surface fluxes and Hα (left) and Ca II λ8498 Å (right). Symbols, colours and line styles as in Fig. 4.

5 NON-UNIVERSALITY OF FLUX–FLUX RELATIONSHIPS

5.1 Two distinct chromospheric emitter populations

Despite having obtained values for the slope of the flux–flux relationships very similar to those found by other authors, a simple visual inspection of Fig. 4 shows that some K-type (circles) and M-type (squares) stars clearly follow a different trend from that observed for other stars in some indicators. The linear relation still holds for these stars (dotted lines) but the slope is different from that obtained when all the stars are considered (see Table 3). The deviation of these stars from the general relationships can be interpreted as an excess of Hα emission with respect to Ca II K (right panel) or Ca II IRT (left panel).

Some authors have previously reported departures of dMe stars from general flux–flux relationships between chromospheric and transition-region indicators (see Oranje 1986), but their sample did not include enough stars to determine whether only dMe stars followed a different trend or whether it was an intrinsic behaviour of late-type stars. Different explanations for this behaviour have been proposed, including a different structure of the atmosphere of dMe stars (Schrijver & Rutten 1987) and a deficiency in the H & K emission with re-radiation in other emission lines (Rutten et al. 1989), although the higher Balmer lines probably do not compensate for the deficiencies observed in other chromospheric lines. Differences in the behaviour of flare dM stars when two chromospheric indicators are compared have been previously suggested, but using a small sample of stars (López-Santiago et al. 2005). This is the first time that a clear departure from the general chromospheric flux–flux relationships is observed for a sufficiently large sample of late-type stars.

It is important to mention here that, in contrast to most previous studies in which the chromospheric component of Hα is taken to be simply the emission flux above a pseudo-continuum (Mohanty & Basri 2003; West et al. 2004, 2008), in this work, Hα equivalent widths were measured in the subtracted spectrum. This fact ensures that the measured fluxes are only chromospheric fluxes, giving full credibility to the deviations observed in the flux–flux relationships.

The peculiar behaviour of these stars extends when we compare X-ray fluxes to those in chromospheric calcium lines (see Fig. 5). Given that X-ray and Hα fluxes present an almost linear relation (see Table 2) it is not surprising that those stars that deviate from the main flux–flux relationships when Hα is one of the diagnostics, also deviate when X-ray emission is considered. Note that Rutten et al. (1989) found that dMe stars deviated from the F_X–$F_{H\alpha}$ relationship. However, in the latter work, they subtracted the contribution of the photosphere in F and G stars but not in M stars.

For the three diagrams in which two branches are clearly observed, we have determined flux–flux relationships for each branch separately. The results are shown in Table 3. Notice that the M stars in Fig. 4 are situated even above the obtained linear fit of the upper branch stars. These stars might follow a slightly different trend. It is important to note that the new relationships for the lower branches show different slopes from those obtained when all the stars are used for the fitting, especially for the most active stars. This difference should be taken into account when working with samples of late-type active stars.

Table 3. Linear fit coefficients for flux–flux relationships with the stars appearing in two different branches.

log F_1	log F_2	Branch	c_1	c_2
Hα	Ca II IRT (λ8498 Å)	Lower	-1.72 ± 0.35	1.33 ± 0.06
		Upper	2.26 ± 0.62	0.71 ± 0.10
Hα	Ca II K	Lower	-2.10 ± 0.85	1.29 ± 0.14
		Upper	3.31 ± 0.43	0.50 ± 0.07
X	Ca II IRT (λ8498 Å)	Lower	-2.84 ± 0.84	1.58 ± 0.15
		Upper	1.39 ± 0.42	1.00 ± 0.07

5.1.1 *Nature of the two populations*

We have investigated the nature of the apparent two populations of chromospheric emitters. In Fig. 6, we plot $\log L_X/L_{bol}$ versus $\log F_{H\alpha}$ and $\log F_{8498}$. The L_X/L_{bol} ratio is a good estimator of magnetic activity in late-type stars. It reaches a maximum $\sim 10^{-2,-3}$ for (very active) high X-ray emitters and decreases to $10^{-5,-6}$ for less magnetically active stars. This behaviour is related to stellar

Downloaded from http://mnras.oxfordjournals.org/ at Universidad Complutense de Madrid on February 9, 2016

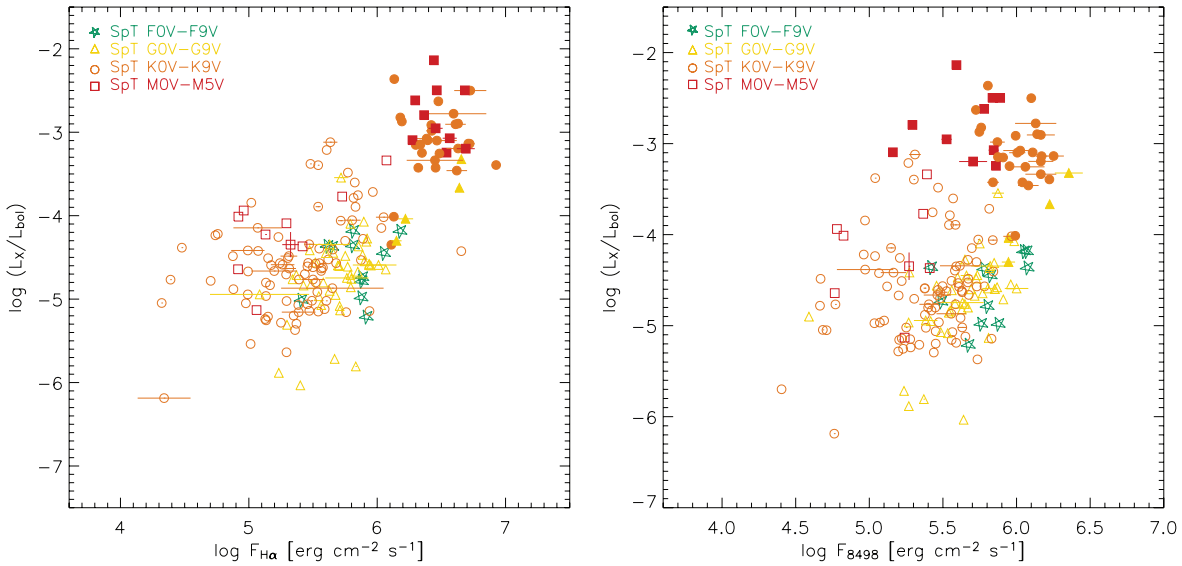

Figure 6. X-ray luminosity versus Hα excess emission (left) and Ca II IRT λ8498 Å (right). Symbols and colours as in Fig. 4.

rotation. It has been observed that X-ray emission in fast rotators is saturated (see Pizzolato et al. 2003, and references therein). This saturation has been proved to be independent of stellar mass and rotation rate (Hempelmann et al. 1995; James et al. 2000). The physical phenomenon behind this saturated regime is still controversial, but the transition boundary between both regimes has been found to be dependent on the rotational period for a given spectral type (Pizzolato et al. 2003), and thus dependent on age because of the time dependence of stellar rotation (Barnes 2003; Mamajek & Hillenbrand 2008). Thus, L_X/L_{bol} can be used as a measure of the level of stellar magnetic activity and an estimator of age. Fig. 6 shows that stars with higher chromospheric Hα surface fluxes are in the X-ray saturation regime. These stars are mainly situated in the upper branch in Fig. 4. Therefore, the stars conforming the upper branch in the Hα–Ca II flux–flux relationships are mainly saturated X-ray emitters. This hypothesis was suggested by López-Santiago et al. (2009) in a study of a sample of young stars that were possible members of young stellar kinematic groups. In that work, the authors observed that there were two well-defined branches of Hα emitters in the $\log F_{H\alpha}$–$(V-I)$ diagram.

To confirm that these stars have rotation rates in agreement with having a saturated X-ray emission, we have compiled the photometric periods when available. We list the values in Table 4. With the exception of HIP 23309, DK Leo and HD 135363, all the upper branch stars for which photometric periods were measured, have $P_{phot} < 4.5$ d. This corresponds to the saturated regime for each mass range according to the results obtained by Pizzolato et al. (2003).

Given that the two-population distribution resembles the segregation observed by Vaughan & Preston (1980) in Ca II H & K, we have studied whether there is a relation between the discrepancy in Hα emission and the position of these stars in a flux–colour diagram like that presented by Vaughan & Preston. We have studied the position of the upper branch stars in an activity–colour index diagram (see left panel in Fig. 7). We have plotted the emission flux in Hα (left) and the total flux in Ca II (right) H & K lines versus $B-V$. There is a clear gap between stars with high Hα emission and those with lower activity levels, particularly for K and M stars. We have used filled symbols to mark these stars in all the plots. We note that those stars in the region on top of the gap in the Hα–$(B-V)$ relation are those that deviate from the general flux–flux relationship between Hα and the calcium lines. Note also that the gap is not as noticeable when the activity index used is the total flux in Ca II H & K instead of Hα, yet those stars with abnormal Hα emission are also in the upper region in this plot. A similar result was found by LS10. In Table 4, we list the stars that belong to the upper branch in Fig. 7. For these, we give values of $\log F_{H\alpha}$ and $\log F_X$.

5.1.2 *Ages and dynamo*

Diagrams such as those presented in Fig. 7 have been interpreted as a result of the rapid decay of the magnetic flux with age rather than a discontinuity in emission levels. The saturation in the chromospheric emission of young stars (Hartmann et al. 1984; Hartmann & Noyes 1987) would result in the concentration of stars above the Vaughan–Preston gap. Therefore, the gap would separate young stars from older stars (Noyes et al. 1984; Zuckerman & Song 2004; Böhm-Vitense 2007; Pace et al. 2009).

Several authors have suggested that the gap actually separates stars with two different dynamo regimes and that this dynamo could change over the star's lifetime. In a recent study, Böhm-Vitense (2007) concludes that there are two different dynamos at work in the two branches observed in the diagram of the cycle period versus rotation period. The existence of two dynamos was previously proposed by Durney, Mihalas & Robinson (1981) as an explanation for the Vaughan–Preston gap. They also suggested that this could produce a change in the morphology of the magnetic field between early-type and late-type stars. Although this interpretation is still controversial, it could be a plausible explanation for the two clearly independent populations of stars that we find when the Hα emission is considered.

To investigate if the upper branch is formed by young stars, we studied age indicators in our sample. In particular, we used data from López-Santiago et al. (2006), LS10, Maldonado et al. (2010), Montes et al. (2001b) and Torres et al. (2008) to determine if the star was a member of a young stellar association or moving group. In Table 4, we give details about the membership of each

Downloaded from http://mnras.oxfordjournals.org/ at Universidad Complutense de Madrid on February 9, 2016

Table 4. Stellar parameters of the stars in the 'upper branch'.

Name	SpT	$B-V$	RA (hh mm ss)	Dec. (deg′ ″)	Source	log $F_{H\alpha}$ (erg cm^{-2} s^{-1})	log F_X (erg cm^{-2} s^{-1})	Notes on the stellar age	P_{phot} (d)	Ref.[a]
PW And	K2V	1.04	00 18 20.89	+30 57 22.2	LS10	6.54 ± 0.06	7.66	AB Dor[b], flare star	1.74	E
QT And	K2V	0.92	00 41 17.34	+34 25 16.9	LS10	6.63 ± 0.07	7.63	Ca, EW (LiI) = 132.2 mÅ [c,d]	2.86	M
BD+17 232	K4V	1.01	01 37 39.42	+18 35 32.9	LS10	6.70 ± 0.11	7.96	LA, EW (LiI) = 405.6 mÅ [c,e], flare star	–	–
V577 Per	K1V	0.70	03 33 13.49	+46 15 26.5	LS10	6.32 ± 0.12	7.34	AB Dor[b]	1.45	J
HD 25457	F6V	0.52	04 02 36.74	−00 16 08.1	LS10	6.18 ± 0.19	6.78	AB Dor[b]	–	–
V834 Tau	K3V	1.10	04 41 18.85	+20 54 05.4	LS10	6.48 ± 0.17	7.15	Uma, EW (LiI) = 56.5 mÅ [c,d], flare star	3.94	J
V1005 Ori	M1.5V	1.41	04 59 34.83	+01 47 00.6	FEROS05	6.30 ± 0.02	7.57	β Pic[f], flare star	4.4	L, O
HIP 23309	M0.5V	1.40	05 00 47.13	−57 15 25.4	FEROS05	6.19 ± 0.02	7.32	β Pic[f]	8.6	L
V371 Ori	M2.5V	1.58	05 33 44.79	+01 56 43.4	FEROS05	6.44 ± 0.01	7.77	YD[g],flare star	–	–
UY Pic B	K5V	0.79	05 36 55.07	−47 57 47.9	FEROS05	6.93 ± 0.04	7.27	AB Dor[b]	4.52	C
AO Men	K4IV	1.13	06 18 28.21	−72 02 41.5	FEROS05	6.48 ± 0.01	7.76	β Pic[f]	2.67	O
BD+20 1790	K5V	1.07	07 23 43.59	+20 24 58.7	LS10	6.62 ± 0.07	6.96	AB Dor[b], flare star	2.8	D, M
V372 Pup	M1.5IV	1.44	07 28 51.37	−30 14 48.5	FEROS05	6.46 ± 0.01	7.64	AB Dor[b]	1.64	G
BD+21 2462	K3V	1.01	07 43 48.49	−36 13 06.5	LS10	6.11 ± 0.23	6.11	IC, EW (LiI) = 40.4 mÅ [c,d]	–	–
YZ CMi	M4.5V	1.61	07 44 40.17	+03 33 08.8	FEROS05	6.68 ± 0.04	7.39	LA[4], flare star	2.78	P
FP Cnc	K7V	1.40	08 08 56.40	+32 49 11.2	LS10	6.18 ± 0.06	7.37	LA[c], flare star	–	–
HD 77407	G0V	0.60	09 03 27.08	+37 50 27.5	LS10	6.22 ± 0.20	6.84	LA, EW (LiI) = 161.3 mÅ [c,d]	–	–
LQ Hya	K0V	0.91	09 32 25.57	−11 11 04.7	MA10/LS10	6.71 ± 0.02	7.40	YD, EW (LiI) = 240.3 mÅ [c,e]	1.60	H, Q
DX Leo	K0V	0.78	09 32 43.76	+26 59 18.7	MA10/LS10	6.13 ± 0.03	6.65	LA, EW (LiI) = 192.4[h,d], 176.3[c,d] mÅ	6	A
DK Leo	K7V	1.24	10 14 19.18	+21 04 29.6	LS10	6.46 ± 0.08	6.90	LA[c], flare star	7.98	N
AD Leo	M3.5V	1.50	10 19 36.28	+19 52 12.1	LS10	6.45 ± 0.08	7.10	Cas[c], flare star	2.60	N
V857 Cen	M4.5V	1.54	11 31 46.51	−41 02 47.2	FEROS05	6.11 ± 0.02	7.97	HS[c], flare star	–	–
EQ Vir	K4V	1.20	13 34 43.21	−08 20 31.3	FEROS05/MA10	6.34 ± 0.01	7.20	IC[c], flare star	3.96	B
EK Dra	G1.5V	0.63	14 39 00.21	+64 17 29.9	LS10	6.46 ± 0.04	7.18	LA, subgroup B4 [b]	2.79	J
IU Dra	G0V	0.67	15 05 49.90	+64 02 49.9	LS10	6.15 ± 0.29	6.50	HS, EW (LiI) = 144.9 mÅ [c,d]	4.45	J
HD 135363	K0V	0.94	15 07 56.26	+76 12 02.7	LS10	6.65 ± 0.07	7.61	HS, EW (LiI) = 198.2 mÅ [c,d]	7.24	G
HD 139751	K3/K4V	1.40	15 40 28.39	−18 41 46.2	FEROS05	6.13 ± 0.02	7.83	AB Dor[b]	3.7	L
CR Dra	M1V	1.24	16 17 05.39	+55 16 09.1	LS10	6.55 ± 0.08	7.25	YD[c], flare star	–	–
V1054 Oph	M4V	1.49	16 55 28.75	−08 20 10.8	FEROS05	6.36 ± 0.01	7.26	HS[c], flare star	–	–
V647 Her	M3.5V	1.46	17 19 54.20	+26 30 03.0	LS10	6.28 ± 0.05	7.02	HS[c], flare star	1.34	J
V889 Her	G2V	0.62	18 34 20.10	18 41 24.2	LS10	6.65 ± 0.15	7.54	LA, EW (LiI) = 208.4 mÅ [c,e]	1.34	F
2RE J1846+191	K4V	1.49	18 46 09.34	+19 12 14.9	LS10	6.12 ± 0.07	–	YD[c]	–	–
LO Peg	K3V	1.03	21 31 01.71	+23 20 07.4	LS10	6.65 ± 0.08	7.25	AB Dor[b]	0.42	I, L
V383 Lac	K1V	0.83	22 20 07.03	+49 30 11.8	LS10	6.44 ± 0.12	7.28	LA, EW (LiI) = 260.0 mÅ [c,e]	2.42	J
GJ 856 B	M1V	1.49	22 23 30.00	+32 27 00.0	LS10	6.54 ± 0.06	–	LA, subgroup B4 [b]	–	–
BD+17 4799	K0V/IV	0.88	22 44 41.54	+17 54 18.3	LS10	6.37 ± 0.12	7.49	LA, EW (LiI) = 247.6 [c,e]	–	–
EV Lac	M3.5V	1.39	22 46 49.73	+44 20 02.4	LS10	6.69 ± 0.04	7.01	LA[c], flare star	4.38	N
GJ 9809	M0V	1.21	23 06 04.84	+63 55 34.4	LS10	6.54 ± 0.05	7.10	AB Dor[b], flare star	4.50	G
V368 Cep	K0V	0.89	23 19 26.63	+79 00 12.7	LS10	6.44 ± 0.10	7.46	LA, EW (LiI) = 205.4 mÅ [c,d]	2.74	H

[a]A, Baliunas, Sokoloff & Soon (1996); B,Bopp & Fekel (1977); C, Cutispoto et al. (1999); D, Hernán-Obispo et al. (2010); E, Hooten & Hall (1990); F, Järvinen et al. (2008); G, Koen & Eyer (2002); H, Kovári et al. (2002); I, Lister, Collier Cameron & Bartus (1999); J, Messina, Rodonó & Guinan (2001); K, Messina et al. (2003); L, Messina et al. (2010); M, Norton et al. (2007); N, Pizzolato et al. (2003); O, Pojmanski (2003); P, Saar (2001); Q, Strassmeier et al. (1997).
[b]López-Santiago et al. (2006).
[c]LS10.
[d]Consistent with the age of the Pleiades: Ca, Castor; HS, Hyades SC; IC, IC2391; LA, Local Association; UMa, Ursa Major MG; YD, young disc.
[e]Consistent with being younger than the Pleiades.
[f]Torres et al. (2008).
[g]Montes et al. (2001b).
[h]Maldonado et al. (2010).

star in the upper branch of Fig. 7 in any young group. From the 39 stars belonging to the upper branch, nine are members of the AB Dor moving group (∼50 Myr; Zuckerman & Song 2004), three are members of the β Pic association (∼12–20 Myr; Barrado y Navascués et al. 1999; Zuckerman & Song 2004) and two stars are members of the subgroup B4 of the Local Association (∼80–120 Myr; López-Santiago et al. 2006).

For those stars in LS10 and MA10, the preliminary membership (based only on their kinematics; see LS10) in young moving groups has been complemented with the information provided by the equivalent width of the Li I 6707.8 Å. The lithium equivalent widths are given in Table 4 and are taken from LS10 and Maldonado et al. (2010). The latter is an indicator of age for young (age $\lesssim\approx$ 650 Myr) stars (see details in Montes et al. 2001a; López-Santiago et al. 2006). For details about the ages of the young moving groups and the technique used to assign a star to a moving group, see LS10.

We note that in most cases there is a good agreement between the kinematic classification and the ages obtained using lithium. Five of these stars (BD+17 232, LQ Hya, V383 Lac, V889 Her and BD+17 4799) have values of EW(Li I) higher than those found for the Pleiades members. The remaining eight stars have equivalent widths compatible with having an age similar to the Pleiades cluster. Finally, two stars, DK Leo and FP Cnc, were assigned to the Local Association moving group, but given that they are late-type stars, their ages could not be confirmed by means of lithium dating (LS10). In addition, the star 2RE J1846+191 was classified as a YD star by means of its kinematics, but its age could not be confirmed by lithium dating (LS10).

Therefore, from the 39 stars in the upper branch, 30 are younger than the Pleiades or have an age similar to that of the latter cluster, confirming the hypothesis that the saturated X-ray regime corresponds to young stars.

Downloaded from http://mnras.oxfordjournals.org/ at Universidad Complutense de Madrid on February 9, 2016

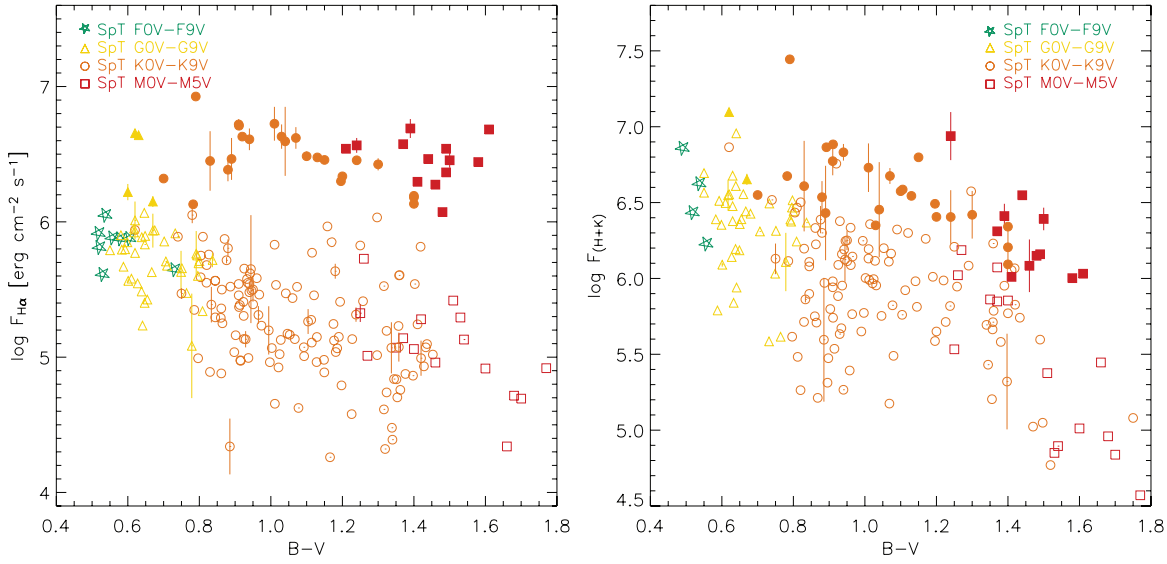

Figure 7. Hα excess emission versus colour index $B - V$ (left). Total excess emission in Ca II H & K versus colour index $B - V$ (right). Filled symbols are used for those stars that conform to the upper region of the gap. Colours as in Fig. 4.

The remaining nine stars in the upper branch in Fig. 7 are dwarf flare (UV Ceti type) stars (see Table 4). We have classified a star as flare when it was included in Gershberg et al. (1999) and/or Pettersen (1991). Some of these have previously been classified as members of a young moving group (Montes et al. 2001b, LS10) although they need spectroscopic confirmation. Nevertheless, whatever their age is, they present enhanced X-ray emission. In fact, they present X-ray emission levels in the saturation regime.

5.1.3 Flare stars

A large fraction (41 per cent) of the stars in the upper branch (see Section 5.1) are well-known M UV Ceti-type flare dwarfs (see Table 4) or K-type flare stars (PW And, BD+17 232, BD+20 1790, DK Leo and FP Cnc) discovered by López-Santiago et al. (2003) and Montes et al. (2005). It is well known that during a flare event, and given that calcium and Balmer lines form at different heights in the stellar atmosphere, the growth of the latter is larger than that of the former (Hawley et al. 2003; Crespo-Chacón et al. 2004, 2006). This fact suggests the idea that flare-like events may be responsible for the different behaviour that these stars show in the flux–flux relationship. So, the question arises: are flare-induced variations compatible with our observations?

Crespo-Chacón et al. (2004,2006) carried out a high temporal resolution spectroscopic monitoring of the stars V1054 Oph and AD Leo. Studying the temporal evolution of the Balmer series and Ca II H & K lines, they detected frequent (>0.71 flares h^{-1}) short and weak non-white-light flares. Some of these events lasted as little as 14 min. Additional observations by Crespo-Chacón et al. (2005) suggest that this kind of frequent short flare is of common occurrence on UV Ceti-type flare stars. In the present work, the observed spectra were obtained using typical exposure times ∼25 min. Thus, one or two of these types of flare events probably occurred on the flare stars during their observation. However, even if this were the case, it would not explain the different behaviour found in the flux–flux relationships between the stars in the upper branch and the others. In fact, Crespo-Chacón et al. (2006) derived (for AD Leo) a value of the order of 10^{30} erg for the energy released in the Hα line by a flare event of the above type with a duration of 30 min. This implies that flares of this type would contribute with a mean Hα surface flux of the order of 10^5 erg cm^{-2} s^{-1}. Thus, one, or even two, of these events taking place on some of the target stars during our observations would only introduce a small increase in their measured line fluxes. This would not explain the whole observed 'deviation' of the stars in the upper branch from the general trend followed by the remainder. Moreover, the clear trend followed by the stars of the upper branch in the flux–flux relationship cannot be the result of events of this type occurring randomly in their atmospheres during the time they were observed.

However, we have detected emission in the He I D_3 line in all the stars classified as flare stars located in the upper branch. In active stars, the He I D_3 line is usually observed in absorption and sometimes in emission, as during flare events (Montes et al. 1997, 1999; García-Alvarez et al. 2003; López-Santiago et al. 2003; Crespo-Chacón et al. 2006). The He I D_3 line at λ5876 Å has a very high excitation level. High temperatures (>15 000 K) and electron densities > 10^{14} cm^{-3} are required to reach emission in this line (Feldman, Liggett & Zirin 1983). Nanoflare heating has been proposed as the main heating mechanism of the stellar outer atmospheres. The energy distribution of flares has been found to be a power law (Datlowe, Elcan & Hudson 1974; Lin et al. 1984) of the form[5] $\mathrm{d}N/\mathrm{d}E = kE^{-\alpha}$. Crespo-Chacón et al. (2006) concluded that very weak flares are expected to occur much more frequently than those observed in that work (> 0.71 flares h^{-1}), in the sense that the quiescent emission of the UV Ceti-type stars in the upper branch may be the result of a superposition of multiple small flares (called nanoflares) following the distribution law given above.

6 SUMMARY AND CONCLUSIONS

In this paper, we present empirical flux–flux power-law relationships between the most important chromospheric activity indicators

[5] In this power law, dN is the number of flares (per unit time) with a total energy (thermal or radiated) in the interval $[E, E + \mathrm{d}E]$ and α is greater than 0 (see section 1 in Crespo-Chacón et al. 2007, for the value of α derived by different authors and its relation with nanoflare heating of quiescent coronae).

Downloaded from http://mnras.oxfordjournals.org/ at Universidad Complutense de Madrid on February 9, 2016

for a large sample of main-sequence F, G, K and M stars. In addition, we obtain relations between X-ray and chromospheric surface fluxes for different chromospheric lines. These new relationships will be useful for comparing classical and present/future data of magnetic activity.

For the first time, we have proved the non-universality of some flux–flux relations between chromospheric indicators. General power laws hold for the majority of the stars, but some late-K and M dwarf stars deviate from the general trend when Hα is used as a chromospheric activity diagnostic. We have also confirmed that this different behaviour persists when X-ray fluxes are used instead of Hα ones. Therefore, late-type stars follow two different power-law flux–flux relationships when X-rays or Hα are used as magnetic activity indicators. We have quantified, for the first time, the departure of these stars from the general trend of other active stars. From their membership in young stellar associations or moving groups and/or lithium abundance, we have shown that most of the stars in the upper branch of the above-mentioned relationships are indeed young stars. This is also confirmed by their position in the $\log F_{\mathrm{H}\alpha}$–$(B-V)$ diagram.

The remaining stars in the upper branch are flare stars. We have proved that a single flare event occurring during the observation cannot account for the deviation observed in the flux–flux relationships. However, a plausible explanation for this deviation may be the hypothesis of nanoflare heating, which suggests that the quiescent state of the star is the result of the superposition of multiple small flares.

Regardless of whether the explanation is the age of the stars or such nanoflare heating, and given that all the upper branch stars are in the (magnetic activity) saturation regime, it is our belief that their different behaviour in the flux–flux relationships is a consequence of a shared physical phenomenon. These stars probably have a magnetic structure that differs in some way from that of the less active stars.

ACKNOWLEDGMENTS

The authors acknowledge support from the Spanish Ministerio de Educación y Ciencia (currently the Ministerio de Ciencia e Innovación), under the grant FPI20061465-00592 (Programa Nacional Formación Personal Investigador) and projects AYA2008-00695 (Programa Nacional de Astronomía y Astrofísica), AstroMadrid S2009/ESP-1496. JL-S acknowledges support by the Spanish Ministerio de Ciencia e Innovación under grant AYA2008-06423-C03-03. This research has made use of the SIMBAD data base and the VizieR catalogue access tool, operated at CDS, Strasbourg, France.

REFERENCES

Baliunas S., Sokoloff D., Soon W., 1996, ApJ, 457, L99
Barden S. C., 1985, ApJ, 295, 162
Barnes S. A., 2003, ApJ, 586, 464
Barrado y Navascués D., Martín E. L., 2003, AJ, 126, 2997
Barrado y Navascués D., Stauffer J. R., Song I., Caillault J., 1999, ApJ, 520, L123
Böhm-Vitense E., 2007, ApJ, 657, 486
Bopp B. W., Fekel F. Jr, 1977, AJ, 82, 490
Busà I., Aznar Cuadrado R., Terranegra L., Andretta V., Gomez M. T., 2007, A&A, 466, 1089
Cincunegui C., Díaz R. F., Mauas P. J. D., 2007, A&A, 469, 309
Crespo-Chacón I., Montes D., Fernández-Figueroa M. J., López-Santiago J., García-Alvarez D., Foing B. H., 2004, Ap&SS, 292, 697
Crespo-Chacón I., Montes D., Fernández-Figueroa M. J., López-Santiago J., 2005, in Favata F., Hussain G. A. J., Battrick B., eds, Proc. 13th Cambridge Workshop on Cool Stars, Stellar Systems and the Sun, ESA Special Publication Vol. 560. ESA, Noordwijk, p. 491
Crespo-Chacón I., Montes D., García-Alvarez D., Fernández-Figueroa M. J., López-Santiago J., Foing B. H., 2006, A&A, 452, 987
Crespo-Chacón I., Micela G., Reale F., Caramazza M., López-Santiago J., Pillitteri I., 2007, A&A, 471, 929
Cuntz M., Saar S. H., Musielak Z. E., 2000, ApJ, 533, L151
Cutispoto G., Pastori L., Tagliaferri G., Messina S., Pallavicini R., 1999, A&AS, 138, 87
Datlowe D. W., Elcan M. J., Hudson H. S., 1974, Solar Physics, 39, 155
Durney B. R., Mihalas D., Robinson R. D., 1981, PASP, 93, 537
Feldman U., Liggett M., Zirin H., 1983, ApJ, 271, 832
García-Alvarez D. et al., 2003, A&A, 397, 285
Gershberg R. E., Katsova M. M., Lovkaya M. N., Terebizh A. V., Shakhovskaya N. I., 1999, A&AS, 139, 555
Hall J. C., 1996, PASP, 108, 313
Hartmann L. W., Noyes R. W., 1987, A&AR, 25, 271
Hartmann L., Soderblom D. R., Noyes R. W., Burnham N., Vaughan A. H., 1984, ApJ, 276, 254
Hawley S. L. et al., 2003, ApJ, 597, 535
Hempelmann A., Schmitt J. H. M. M., Schultz M., Ruediger G., Stepien K., 1995, A&A, 294, 515
Henry G. W., Baliunas S. L., Donahue R. A., Soon W. H., Saar S. H., 1997, ApJ, 474, 503
Hernán-Obispo M., Gálvez-Ortiz M. C., Anglada-Escudé G., Kane S. R., Barnes J. R., de Castro E., Cornide M., 2010, A&A, 512, A45
Hooten J. T., Hall D. S., 1990, ApJS, 74, 225
Huenemoerder D. P., Barden S. C., 1984, BAAS, 16, 510
Isobe T., Feigelson E. D., Akritas M. G., Babu G. J., 1990, ApJ, 364, 104
James D. J., Jardine M. M., Jeffries R. D., Randich S., Collier Cameron A., Ferreira M., 2000, MNRAS, 318, 1217
Järvinen S. P., Korhonen H., Berdyugina S. V., Ilyin I., Strassmeier K. G., Weber M., Savanov I., Tuominen I., 2008, A&A, 488, 1047
Jenkins J. S., Ramsey L. W., Jones H. R. A., Pavlenko Y., Gallardo J., Barnes J. R., Pinfield D. J., 2009, ApJ, 704, 975
Koen C., Eyer L., 2002, MNRAS, 331, 45
Kovári Z., Strassmeier K. G., Granzer T., Weber M., Oláh K., Rice J. B., 2004, A&A, 417, 1047
Lin R. P., Schwartz R. A., Kane S. R., Pelling R. M., Hurley K. C., 1984, ApJ, 283, 421
Lister T. A., Collier Cameron A., Bartus J., 1999, MNRAS, 307, 685
López-Santiago J., 2005, PhD thesis, Universidad Complutense de Madrid
López-Santiago J., Montes D., Fernández-Figueroa M. J., Ramsey L. W., 2003, A&A, 411, 489
López-Santiago J., Montes D., Fernández-Figueroa M. J., Gálvez M. C., Crespo-Chacón I., 2005, in Favata F., Hussain G. A. J., Battrick B., eds, Proc. 13th Cambridge Workshop on Cool Stars, Stellar Systems and the Sun, ESA Special Publication Vol. 560. ESA, Noordwijk, p. 775
López-Santiago J., Montes D., Crespo-Chacón I., Fernández-Figueroa M. J., 2006, ApJ, 643, 1160
López-Santiago J., Micela G., Montes D., 2009, A&A, 499, 129
López-Santiago J., Montes D., Gálvez-Ortiz M. C., Crespo-Chacón I., Martínez-Arnáiz R. M., Fernández-Figueroa M. J., de Castro E., Cornide M., 2010, A&A, 514, A97 (LS10)
Maldonado J., Martínez-Arnáiz R. M., Eiroa C., Montes D., Montesinos B., 2010, A&A, 521, A12
Mamajek E. E., Hillenbrand L. A., 2008, ApJ, 687, 1264
Martínez-Arnáiz R., Maldonado J., Montes D., Eiroa C., Montesinos B., 2010, A&A, 520, A79 (MA10)
Messina S., Rodonò M., Guinan E. F., 2001, A&A, 366, 215
Messina S., Pizzolato N., Guinan E. F., Rodonò M., 2003, A&A, 410, 671
Messina S., Desidera S., Turatto M., Lanzafame A. C., Guinan E. F., 2010, A&A, 520, A15
Mohanty S., Basri G., 2003, ApJ, 583, 451

Downloaded from http://mnras.oxfordjournals.org/ at Universidad Complutense de Madrid on February 9, 2016

Montes D., de Castro E., Fernández-Figueroa M. J., Cornide M., 1995a, A&AS, 114, 287
Montes D., Fernández-Figueroa M. J., de Castro E., Cornide M., 1995b, A&A, 294, 165
Montes D., Fernández-Figueroa M. J., Cornide M., de Castro E., 1996a, in Pallavicini R., Dupree A. K., eds, ASP Conf. Ser. Vol. 109, Cool Stars, Stellar Systems, and the Sun. Astron. Soc. Pac., San Francisco, p. 657
Montes D., Fernández-Figueroa M. J., Cornide M., de Castro E., 1996b, A&A, 312, 221
Montes D., Fernández-Figueroa M. J., de Castro E., Sanz-Forcada J., 1997, A&AS, 125, 263
Montes D., Saar S. H., Collier Cameron A., Unruh Y. C., 1999, MNRAS, 305, 45
Montes D., Fernández-Figueroa M. J., de Castro E., Cornide M., Latorre A., Sanz-Forcada J., 2000, A&AS, 146, 103
Montes D., López-Santiago J., Fernández-Figueroa M. J., Gálvez M. C., 2001a, A&A, 379, 976
Montes D., López-Santiago J., Gálvez M. C., Fernández-Figueroa M. J., de Castro E., Cornide M., 2001b, MNRAS, 328, 45
Montes D., López-Santiago J., Crespo-Chacón I., Fernández-Figueroa M. J., 2005, in Favata F., Hussain G. A. J., Battrick B., eds, Proc. 13th Cambridge Workshop on Cool Stars, Stellar Systems and the Sun, ESA Special Publication Vol. 560. ESA, Noordwijk, p. 825
Montes D., López-Santiago J., Crespo-Chacón I., Martínez-Arnáiz R., Maldonado J., 2007, in Highlights of Spanish Astrophysics IV, Proceedings of the VII Scientific Meeting of the Spanish Astronomical Society (SEA). Springer, Berlin
Montes D., López-Santiago J., Crespo-Chacón I., Martínez-Arnáiz R., Maldonado J., 2008, in ASP Conf. Ser. Vol. 384, Cool Stars, Stellar Systems and the Sun. Astron. Soc. Pac., San Francisco
Norton A. J. et al., 2007, A&A, 467, 785
Noyes R. W., Hartmann L. W., Baliunas S. L., Duncan D. K., Vaughan A. H., 1984, ApJ, 279, 763
Oranje B. J., 1986, A&A, 154, 185
Pace G., Melendez J., Pasquini L., Carraro G., Danziger J., Frančois P., Matteucci F., Santos N. C., 2009, A&A, 499, L9
Pettersen B. R., 1991, Mem. della Soc. Astron. Ital., 62, 217
Pizzolato N., Maggio A., Micela G., Sciortino S., Ventura P., 2003, A&A, 397, 147
Pojmanski G., 2003, Acta Astron., 53, 341
Robinson R. D., Cram L. E., Giampapa M. S., 1990, ApJS, 74, 891
Rutten R. G. M., Zwaan C., Schrijver C. J., Duncan D. K., Mewe R., 1989, A&A, 219, 239
Rutten R. G. M., Schrijver C. J., Lemmens A. F. P., Zwaan C., 1991, A&A, 252, 203
Saar S. H., 2001, in García Lopez R. J., Rebolo R., Zapaterio Osorio M. R., eds, ASP Conf. Ser. Vol. 223, Cool Stars, Stellar Systems and the Sun. Astron. Soc. Pac., San Francisco, p. 292
Saar S. H., Donahue R. A., 1997, ApJ, 485, 319
Schmitt J. H. M. M., Fleming T. A., Giampapa M. S., 1995, ApJ, 450, 392
Schrijver C. J., 1987, A&A, 172, 111
Schrijver C. J., Rutten R. G. M., 1987, A&A, 177, 143
Schrijver C. J., Zwaan C., 1991, A&A, 251, 183
Schrijver C. J., Zwaan C., 2000, Solar and Stellar Magnetic Activity, Cambridge Astrophysics Series, 34. Cambridge Univ. Press, Cambridge
Schrijver C. J., Cote J., Zwaan C., Saar S. H., 1989, ApJ, 337, 964
Schrijver C. J., Dobson A. K., Radick R. R., 1992, A&A, 258, 432
Strassmeier K. G., Fekel F. C., Bopp B. W., Dempsey R. C., Henry G. W., 1990, ApJS, 72, 191
Strassmeier K. G., Bartus J., Cutispoto G., Rodonó M., 1997, A&AS, 125, 11
Thatcher J. D., Robinson R. D., 1993, MNRAS, 262, 1
Torres C. A. O., Quast G. R., Melo C. H. F., Sterzik M. F., 2008, in Handbook of Star-Forming Regions, Vol. II: The Southern Sky. ASP Monograph Publications, Vol. 5. Astron. Soc. Pac., San Francisco, p. 757
Vaughan A. H., Preston G. W., 1980, PASP, 92, 385
Walkowicz L. M., Hawley S. L., West A. A., 2004, PASP, 116, 1105
West A. A., Hawley S. L., 2008, PASP, 120, 1161
West A. A. et al., 2004, AJ, 128, 426
West A. A., Walkowicz L. M., Hawley S. L., 2005, PASP, 117, 706
West A. A., Hawley S. L., Bochanski J. J., Covey K. R., Reid I. N., Dhital S., Hilton E. J., Masuda M., 2008, AJ, 135, 785
Zuckerman B., Song I., 2004, A&AR, 42, 685

APPENDIX A: TABLES OF RESULTS

The stellar and line parameters are published as an appendix. Table A1 contains the name of the star (column 1), the right ascension and declination (columns 2 and 3), the spectral type (column 4), the colour index ($B - V$; column 5) and any important note on each star (column 6).

The chromospheric activity results are listed in two different tables. Table A2 contains the excess emission EW as measured in the subtracted spectrum, whereas Table A3 includes the excess fluxes derived in this paper. In both tables, column 1 is the name of the star and columns 2, 3, 4, 5 and 6 give the excess emission (or fluxes) for Ca II K, Ca II H, Hα, Ca II IRT λ8498Å and Ca II IRT λ8662Å; in Table A2, column 7 gives He I D_3.

Table A1. Stellar parameters for the FEROS05 stars.

Name	RA (hhmmss)	Dec. (deg)	SpT	$B - V$
V1005 Ori	04 59 34.83	+01 47 00.7	M1.5V	1.41
HIP 23309	05 00 47.13	−57 15 25.5	M0.5V	1.40
HD 35650	05 24 30.17	−38 58 10.8	K4V	1.25
V371 Ori	05 33 44.79	+01 56 43.4	M2.5V	1.58
UY Pic B	05 36 55.07	−47 57 47.9	K5V	0.79
AO Men	06 18 28.21	−72 02 41.5	K4IV	1.13
HIP 31878	06 39 50.02	−61 28 41.5	M0V	1.26
V372 Pup	07 28 51.37	−30 14 48.5	M1.5IV	1.44
YZ CMi	07 44 40.17	+03 33 08.8	M4.5V	1.61
FR Cnc	08 32 30.53	+15 49 26.2	K8V	1.16
GJ 382	10 12 17.67	−03 44 44.4	M1.5V	1.51
EE Leo	10 50 52.06	+06 48 29.3	M3.5V	1.68
V857 Cen	11 31 46.51	−41 02 47.2	M4.5V	1.54
FI Vir	11 47 44.40	+00 48 16.4	M4V	1.77
EQ Vir	13 34 43.21	−08 20 31.3	K4V	1.20
CE Boo	14 54 29.24	+16 06 03.8	M2.5V	1.48
HD 139751	15 40 28.39	−18 41 46.2	K4V	1.40
V2306 Oph	16 30 18.06	−12 39 45.3	M3.5V	1.60
GJ 643	16 55 25.22	−08 19 21.3	M4V	1.70
V1054 Oph	16 55 28.75	−08 20 10.8	M4V	1.49
GJ 674	17 28 39.95	−46 53 42.7	M2.5V	1.53

Downloaded from http://mnras.oxfordjournals.org/ at Universidad Complutense de Madrid on February 9, 2016

Table A2. Excess emission in different chromospheric activity indicator lines for the active stars in the sample.

Name	Equivalent width (Å) in the subtracted spectrum					
	Ca II			Ca II IRT		
	K	H	Hα	λ8498	λ8662	He I D3
V1005 Ori	2.100 ± 0.230	1.900 ± 0.200	1.940 ± 0.030	0.460 ± 0.010	0.591 ± 0.012	0.054 ± 0.036
HIP 23309	4.590 ± 0.050	3.600 ± 0.040	1.490 ± 0.020	0.420 ± 0.010	0.401 ± 0.010	0.023 ± 0.014
HD 35650	1.680 ± 0.020	1.350 ± 0.020	0.440 ± 0.010	0.220 ± 0.010	0.273 ± 0.007	–
V371 Ori	4.830 ± 0.200	3.740 ± 0.160	4.150 ± 0.030	0.390 ± 0.010	0.440 ± 0.016	0.305 ± 0.062
UY Pic B	3.510 ± 0.030	2.790 ± 0.020	1.760 ± 0.010	0.480 ± 0.010	0.636 ± 0.105	–
AO Men	1.940 ± 0.060	1.840 ± 0.040	1.460 ± 0.020	0.260 ± 0.050	–	–
HIP 31878	1.120 ± 0.040	0.940 ± 0.040	0.360 ± 0.010	0.140 ± 0.010	0.160 ± 0.010	–
V372 Pup	9.070 ± 0.040	6.780 ± 0.020	3.080 ± 0.020	0.550 ± 0.010	0.604 ± 0.007	0.239 ± 0.020
YZ CMi	4.550 ± 0.200	5.970 ± 0.170	7.790 ± 0.040	0.810 ± 0.080	–	0.757 ± 0.062
FR Cnc	5.835 ± 0.575	5.389 ±0.316	1.600 ± 0.022	0.601 ± 0.048	0.576 ± 0.090	0.895 ± 0.385
GJ 382	0.850 ± 0.040	0.620 ± 0.050	0.330 ± 0.020	0.230 ± 0.040	–	–
EE Leo	0.730 ± 0.200	0.500 ± 0.100	0.100 ± 0.030	0.050 ± 0.020	0.099 ± 0.013	–
V857 Cen	–	8.360 ± 0.090	4.600 ± 0.030	0.390 ± 0.050	0.273 ± 0.007	0.382 ± 0.021
FI Vir	0.480 ± 0.150	0.280 ± 0.180	0.200 ± 0.030	0.090 ± 0.020	0.194 ± 0.016	–
EQ Vir	2.090 ± 0.030	1.700 ± 0.020	1.260 ± 0.010	0.410 ± 0.010	0.052 ± 0.011	0.037 ± 0.014
CE Boo	4.320 ± 0.010	3.280 ± 0.040	1.380 ± 0.010	0.210 ± 0.010	0.304 ± 0.009	0.094 ± 0.018
HD 139751	2.590 ± 0.020	2.030 ± 0.030	1.300 ± 0.020	0.480 ± 0.010	0.519 ± 0.012	–
V2306 Oph	0.600 ± 0.160	0.360 ± 0.190	0.130 ± 0.020	0.060 ± 0.030	0.070 ± 0.015	–
GJ 643	0.730 ± 0.240	0.290 ± 0.130	0.100 ± 0.010	0.050 ± 0.030	0.075 ± 0.008	–
V1054 Oph	5.080 ± 0.070	3.070 ± 0.040	2.780 ± 0.030	0.170 ± 0.020	0.180 ± 0.007	0.111 ± 0.034
GJ 674	0.340 ± 0.040	0.140 ± 0.040	0.260 ± 0.020	–	0.099 ± 0.009	–

Table A3. Logarithmic excess surface flux in different chromospheric activity indicator lines for the active stars in the sample.

Name	$\log F_s$ in the subtracted spectrum				
	Ca II			Ca IIIRT	
	K	H	Hα	λ8498	λ8662
V1005 Ori	5.730 ± 0.048	5.687 ± 0.048	6.296 ± 0.020	5.780 ± 0.019	5.889 ± 0.018
HIP 23309	6.090 ± 0.005	5.984 ± 0.005	6.192 ± 0.017	5.747 ± 0.021	5.727 ± 0.021
HD 35650	5.953 ± 0.005	5.858 ± 0.005	5.825 ± 0.030	5.569 ± 0.039	5.663 ± 0.021
V371 Ori	5.753 ± 0.018	5.642 ± 0.018	6.442 ± 0.009	5.592 ± 0.022	5.645 ± 0.031
UY Pic B	7.190 ± 0.004	7.091 ± 0.004	6.926 ± 0.007	6.223 ± 0.018	6.345 ± 0.144
AO Men	6.254 ± 0.013	6.231 ± 0.013	6.476 ± 0.018	5.724 ± 0.167	–
HIP 31878	5.757 ± 0.016	5.680 ± 0.016	5.727 ± 0.036	5.366 ± 0.062	5.425 ± 0.055
V372 Pup	6.306 ± 0.002	6.179 ± 0.002	6.464 ± 0.008	5.837 ± 0.016	5.878 ± 0.011
YZ CMi	5.667 ± 0.019	5.785 ± 0.019	6.683 ± 0.007	5.889 ± 0.086	–
FR Cnc	5.141 ± 0.015	5.173 ± 0.012	6.072 ± 0.007	6.513 ± 0.005	6.519 ± 0.006
GJ 382	5.138 ± 0.020	5.001 ± 0.020	5.418 ± 0.079	5.410 ± 0.151	–
EE Leo	4.733 ± 0.119	4.568 ± 0.119	4.715 ± 0.391	4.631 ± 0.347	4.929 ± 0.116
V857 Cen	5.432 ± 0.006	5.293 ± 0.006	6.107 ± 0.008	5.352 ± 0.111	5.196 ± 0.022
FI Vir	4.371 ± 0.136	4.137 ± 0.136	4.919 ± 0.195	4.825 ± 0.193	5.158 ± 0.070
EQ Vir	6.147 ± 0.006	6.057 ± 0.006	6.336 ± 0.010	5.874 ± 0.021	4.974 ± 0.190
CE Boo	5.904 ± 0.001	5.784 ± 0.001	6.072 ± 0.009	5.391 ± 0.041	5.552 ± 0.024
HD 139751	5.841 ± 0.003	5.735 ± 0.003	6.133 ± 0.020	5.805 ± 0.018	5.840 ± 0.019
V2306 Oph	4.807 ± 0.116	4.585 ± 0.116	4.916 ± 0.200	4.765 ± 0.434	4.830 ± 0.186
GJ 643	4.693 ± 0.143	4.292 ± 0.143	4.694 ± 0.130	4.617 ± 0.521	4.793 ± 0.095
V1054 Oph	5.954 ± 0.006	5.736 ± 0.006	6.365 ± 0.014	5.293 ± 0.102	5.318 ± 0.034
GJ 674	4.700 ± 0.051	4.315 ± 0.051	5.293 ± 0.100	–	5.029 ± 0.082

This paper has been typeset from a TEX/LATEX file prepared by the author.

Downloaded from http://mnras.oxfordjournals.org/ at Universidad Complutense de Madrid on February 9, 2016